Plant, Cell & Environment

Plant, Cell and Environment (2010) **33**, 816–827 doi: 10.1111/j.1365-3040.2009.02108.x

Signal transduction in *Mimosa pudica*: biologically closed electrical circuits

ALEXANDER G. VOLKOV[1], JUSTIN C. FOSTER[1] & VLADISLAV S. MARKIN[2]

[1]Department of Chemistry and Biochemistry, Oakwood University, Huntsville, AL 35896, USA, and [2]Department of Neurology, University of Texas, Southwestern Medical Center, Dallas, TX 75390-8833, USA

ABSTRACT

Biologically closed electrical circuits operate over large distances in biological tissues. The activation of such circuits can lead to various physiological and biophysical responses. Here, we analyse the biologically closed electrical circuits of the sensitive plant *Mimosa pudica* Linn. using electrostimulation of a petiole or pulvinus by the charged capacitor method, and evaluate the equivalent electrical scheme of electrical signal transduction inside the plant. The discharge of a 100 μF capacitor in the pulvinus resulted in the downward fall of the petiole in a few seconds, if the capacitor was charged beforehand by a 1.5 V power supply. Upon disconnection of the capacitor from Ag/AgCl electrodes, the petiole slowly relaxed to the initial position. The electrical properties of the *M. pudica* were investigated, and an equivalent electrical circuit was proposed that explains the experimental data.

Key-words: charged capacitor method; electrical signalling; motor cells; plant electrophysiology.

Abbreviations: *C*, capacitance; DPDT, double-pole double-throw switch; PXI, PCI extensions for instrumentation; *Q*, charge of capacitor; *R*, resistance; *t*, time; *U*, voltage.

INTRODUCTION

Mimosa pudica Linn. is a thigmonastic or seismonastic plant in which the leaves close and the petiole hangs down in response to certain stressors such as a wound, wind, vibration, touch, hot or cold stimulus, drought or change in illumination (Bose 1913, 1918). The unique anatomy of the *M. pudica* contributes to the response mechanism of the plant (Fig. 1). The plant contains long, slender branches called petioles, which can fall because of mechanical, thermal or electrical stimulus. The petioles contain smaller pinnae, arranged on the midrib of the pinna. Pinnules are the smallest leaflets, while the entire leaf contains petioles, pinnae and pinnules. A pulvinus is a joint-like thickening at the base of a plant leaf or leaflet that facilitates thigmonastic movements. Primary, secondary and tertiary pulvini are responsible for the movement of the petiole, pinna and leaflets, respectively (Shimmen 2006).

Correspondence: A. G. Volkov. Fax: +(256) 726-7113; e-mail: agvolkov@yahoo.com

While the mechanism of thigmonastic movement in *M. pudica* is not clear at the present time, there are a few hypotheses. One such hypothesis states that the thigmonastic movement of *M. pudica* is powered by a sudden loss of turgor pressure in the motor cells of the pulvinus at the base of each leaf or leaflet (Bose 1918; Temmei *et al.* 2005). Through the usage of nuclear magnetic resonance, it was possible to observe the movement of water from the lower half of the pulvinus to the upper half of the pulvinus following a mechanical stimulus (Tamiya *et al.* 1988).

There is an opinion that ATPase activity is strongly involved in the thigmonastic movement of *M. pudica* (Liubimova, Deminovskaya & Fedorovich 1964; Liubimova-Engel'gardt *et al.* 1978), and a high density of H^+-ATPase in the phloem and pulvini was found (Fleurat-Lessard *et al.* 1997).

Balmer & Franks (1975) found that the seismonastic movement of *M. pudica*'s petiole after electrostimulation by 200–400 V between soil and a pulvinus is comparable to typical animal muscle movements. The actin cytoskeleton in the pulvinus plays an important role in the petiole bending. Kameyama *et al.* (2000) found that the actin in *M. pudica* is heavily tyrosine phosphorylated, and that changes in the extent of phosphorylation correlate with the degree of bending of the plant's petioles. Ion channels in the pulvinus are involved in the redistribution of potassium, chloride and calcium ions during the gravitotropically induced movement of *M. pudica* (Roblin & Fleurate-Lessard 1987). The contractile characteristics were found to be remarkably similar to those of intact animal muscle (Balmer & Franks 1975). Yao, Xu & Yuan (2008) demonstrated that depolymerization of the actin cytoskeleton in the pulvinus in response to electrical signals resulted in increased levels of calcium concentration.

Thigmonastic or seismonastic movements, such as response to touch, appear to be regulated by electrical and chemical signal transduction, spreading the stimulus throughout the plant (Kagawa & Saito 2000). Electrical signals can induce chemical processes, which were described by Ricca (1916) in the chemical transmission hypothesis. The action potentials that occur in plants have many of the same properties as the action potentials that occur in animals (Bose 1902, 1907, 1926, 1928; Houwink 1938; Volkov 2000; Volkov *et al.* 2007). These properties include the all-or-none law, threshold potentials and refractory periods. The transmission of an action potential induced by a gentle touch is

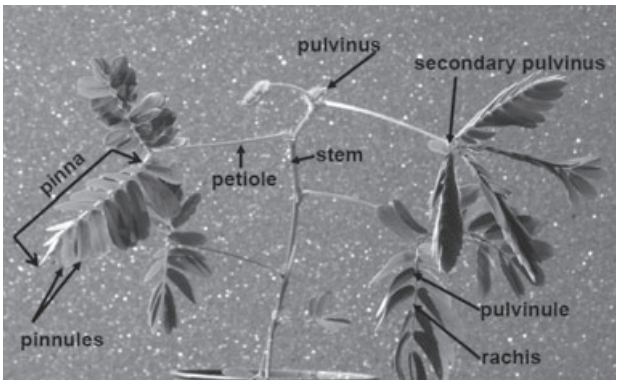

Figure 1. The structure of *Mimosa pudica*.

halted at the base of a single pinna, and no further transmission occurs, leaving leaflets from neighbouring pinna unfolded (Shimmen 2006). Action potentials propagate in the phloem and protoxylem parenchyma of *M. pudica* (Houwink 1938; Sibaoka 1962). The cell's depolarization results from a Cl^- efflux followed by a K^+ efflux, which initiates the repolarization phase (Sibaoka 1991).

According to Shimmen (2006), there are three types of electrical signalling in *M. pudica*: *m*-wave with an action potential speed of 1.5–4 cm s^{-1}, which cannot pass through the pulvinus; *s*-wave or variation potential with a speed of 0.2–0.5 cm s^{-1}; and *r*-wave with a speed of 6–12 cm s^{-1}. As shown in Table 1, literature data on electrical signalling in *M. pudica* have very significant discrepancies between different groups of researchers and even between different publications from the same group. The reasoning behind why there is such difference in amplitude, speed and duration of action potentials could not be found in any publication. The electrical signals in *M. pudica* were usually measured by a single differential voltmeter, but it is not clear if they follow the all-or-nothing law, and their threshold potentials and refractory periods remain unknown. The stimulation of a pinna by a flame generates electrical signals, which are not action potentials because the resting potential did not return back to the initial value after propagation of the electrical signal (Koziolek *et al.* 2003). Fromm & Lautner (2007) reported that cooling or mechanically touching the pinna evoked action potentials with an amplitude of 150 mV, a 5 s duration time and a speed of 2–3 cm s^{-1}. According to literature, the amplitude of action potentials varies from 16 to 210 mV, and the duration of electrical signals varies from 1.2 to 2000 s (Table 1).

There are a few possible reasons for this strange discrepancy including but not limited to: (1) aliasing caused by a low scanning rate of data acquisition systems without low-pass filters or with slow voltmeters with a resolution of 20–100 ms; (2) slow ion-sensitive electrodes with membranes; and (3) high impedance of *M. pudica* tissue which does not permit the use of fast oscilloscopes or high-speed data acquisition systems with a low input impedance. While

Table 1. Electrical signals (action potentials) in *Mimosa pudica*

	Amplitude (mV)	Duration (s)	Speed (cm s^{-1})	Length (cm)	Reference
1	20	5	?	?	Abe 1980
2	20	10	?	?	Abe 1981
3	100	>15	?	?	Abe & Oda 1976
4	145	8	?	?	Fromm 1991
5	140	7–10	?	?	Fromm & Eschrich 1988
6	150	5	2–3	10–15	Fromm & Lautner 2007
7	?	15	2	?	Houwink 1935
8	&	150	?	?	Houwink 1938
9	150	>750	?	?	Kaiser & Grams 2006
10	80–100 electrical signals	>300	0.4–0.8	>120	Koziolek *et al.* 2003
11	100	2.5	?	?	Oda & Abe 1972
12	40–70	5	4	20	Oda & Abe 1972
13	100	15	?	?	Roblin 1979
14	57 ± 16	1770 ± 300	?	?	Roblin 1982
15	119 ± 20	780 ± 120	?	?	Roblin 1982
16	16 ± 7	1890 ± 420	?	?	Roblin 1982
17	105 ± 14	900 ± 60	?	?	Roblin 1982
18	120	4	2–3	?	Sibaoka 1966
19	140 ± 12	3	2–3	6–9	Sibaoka 1962
20	141 ± 15	5	2–3	10–15	Sibaoka 1962
21	80	?	0.3–0.7	?	Sibaoka 1969
22	60	?	4–5	?	Sibaoka 1969
23	110, 170	>5	?	?	Sibaoka 1991
24	210	1.2	?	?	Stoeckel & Takeda 1993
25	100	7	?	?	Tinz-Füchtmeier & Gradmann 1990
26	60	?	4–5	?	Umrath 1937
27	140	7–10	2.7	19–27	Eschrich 1989

the effect of aliasing on the reproducibility of action potentials measurements in plants was discussed in detail by Lang & Volkov (2008), electrical signalling in *M. pudica* requires additional study. It is possible that various stimuli generate different electrical signals in the pulvinus, stem and leaves of *M. pudica*.

Plants can react to mechanical stimuli by using mechanosensitive channels. These channels are found in the cells of various types of organisms – animal, plant, fungal and bacterial. The omnipresence of these channels indicates their important physiological function in the regulation of osmolarity, cell volume and growth. They are ideal transducers of physiologically relevant mechanical forces (Markin & Sachs 2004). Mechanosensory ion channels in plants are activated by mechanical stress, and transduce the sensed information into electrical signals. In higher plants, these channels can be involved in response to environmental stress (Markin, Volkov & Jovanov 2008; Volkov, Carrell & Markin 2009b).

Plants have evolved sophisticated systems to sense environmental stimuli for adaptation, as well as to sense signals from other cells for coordinated action (Trewavas 2003, 2005; Volkov 2006a,b; Volkov & Brown 2006a,b; Volkov *et al.* 2008a; Volkov, Coopwood & Markin 2008b). Plants synchronize their normal biological functions and their responses to the environment (Bertholon 1783; Barlow 2008). The bioelectrochemical systems in plants not only regulate stress responses, but photosynthetic processes as well (Bulychev, Niyazova & Turovetsky 1986; Koziolek *et al.* 2003; Pikulenko & Bulychev 2005; Volkov & Brown 2006a,b). The synchronization of internal functions based on external events is linked to the phenomenon of excitability in plant cells. The generation of electrochemical fluxes is a fundamental aspect of signal transduction. Ion channels are responsible for the transduction of mammalian and plant action potentials. In plants, these potentials can be induced through mechanical stimulation, changing the direction of light (phototropism and heliotropism), chemical treatment, electrostimulation and plant–insect interaction (Volkov & Haack 1995). Most plants respond to mechanical stimuli, and those with rapid and highly noticeable touch-stimulated responses have received much attention, such as the Venus flytrap (*Dionaea muscipula* Ellis) (Darwin 1875; Volkov *et al.* 2007, 2008a,b, 2009a,b,c; Markin *et al.* 2008) or *M. pudica* (Bose 1907, 1918, 1926; Malone 1994; 1996; Fleurat-Lessard *et al.* 1997, Yao *et al.* 2008).

In the study reported, we analysed the biologically closed electrical circuits in *M. pudica* through electrostimulation of the pulvinus and petiole using new charged capacitor method (Volkov *et al.* 2007, 2008a,b, 2009a,b,c). We then evaluated an equivalent electrical scheme of the electrical signal transduction inside this plant.

MATERIALS AND METHODS

Data acquisition

A PXI-4071 digital multimeter (National Instruments, Austin, TX, USA) connected to 0.2-mm-thick non-polarizable reversible Ag/AgCl electrodes was used to record the digital data (Fig. 2). The PXI-4071

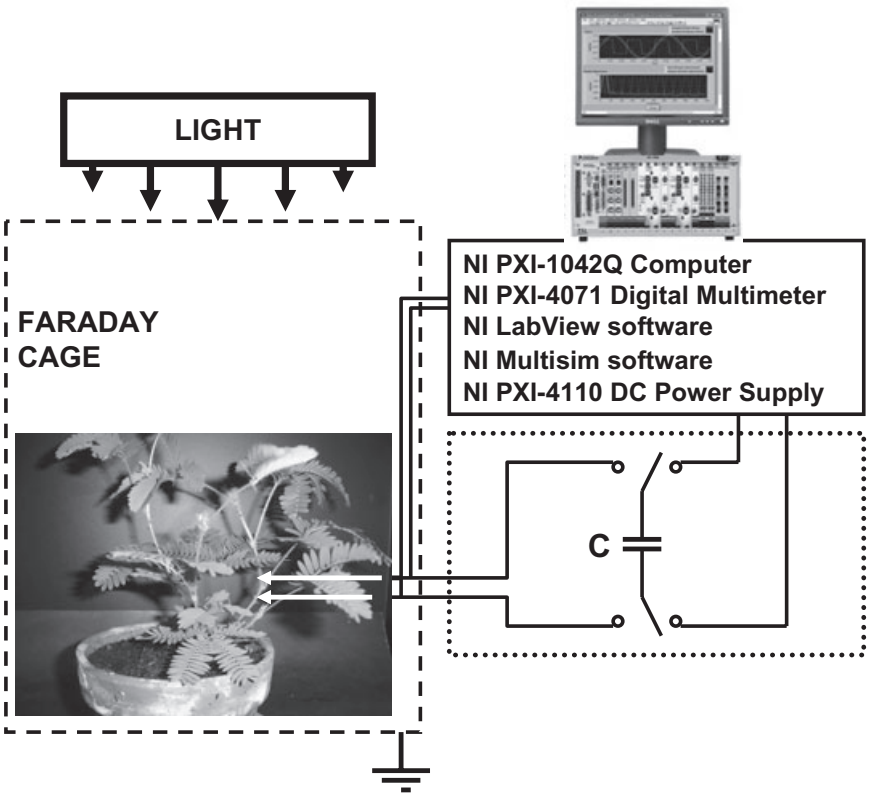

Figure 2. Experimental set-up.

high-resolution digital multimeter delivers fast voltage measurements from 10 nV to 1000 V, current measurements from 1 pA to 3 A and resistance measurements from 10 $\mu\Omega$ to 5 GΩ. All measurements were conducted in the laboratory at 21 °C inside a Faraday cage mounted on a vibration-stabilized table (Fig. 2). Ag/AgCl electrodes were prepared from Teflon-coated wires (A-M Systems, Inc., Sequim, WA, USA) according to the method described by Ksenzhek & Volkov (1998). The response time of Ag/AgCl electrodes was less than 0.1 μs. The time dependencies of the electrical discharge of the capacitor in *M. pudica* were measured between 3 and 20 h after insertion of the electrodes.

Plant electrostimulation

The charge injection method (Volkov *et al.* 2008a,b) was used to precisely estimate the amount of electrical energy necessary to induce a response. A DPDT switch was used to connect the known capacitor to the PXI-4110 DC power supply (National Instruments) during charging, and then to the plant during plant stimulation. By changing the switch position, we can instantaneously connect the charged capacitor to the plant and induce a response. We used various capacitors that had a capacitance ranging from 1–100 μF. Multisim software from National Instruments was used for simulation of electrical circuits in *M. pudica*.

Plants

The seeds of *M. pudica* L. were soaked in warm water (30 °C) for 48 h. They were then grown in well-drained peat moss at 21 °C with a 12:12 h light:dark photoperiod. After growing for 2 weeks, the seedlings were transplanted into pots and placed in a plant-growing chamber. Humidity averaged 45–50%, and the plants were watered every day. Two- to three-month-old plants were used for the experiments. Irradiance was 700–800 μE m^{-2} s^{-1}. All of the experiments were performed on healthy adult specimens.

RESULTS

Capacitor discharge

Figure 3 shows the location of Ag/AgCl electrodes in *M. pudica*. Figures 4a and 5a show the time dependencies of charged capacitors discharging in the petiole of *M. pudica* when the polarity of the same electrodes was reversed.

Figures 6a and 7a show the time dependencies of charged capacitors discharging in the *M. pudica* pulvinus between electrodes located along the pulvinus (Fig. 3a). The kinetics of the capacitor discharge (Figs 6a & 7a) depends on the polarity of the electrodes. If a positive electrode is located near a stem, the capacitor discharge is faster.

Figures 8a and 9a show the time dependencies of charged capacitors discharging in *M. pudica* between electrodes located across a pulvinus. If a positive electrode is located on top of the pulvinus (Figs 3b & 9a), the capacitor discharge is faster than in the case of a negative electrode being on top of a pulvinus (Figs 3b & 8a). Figure 9a shows a very unusual shape of a capacitor discharge with variable curvature of the curve.

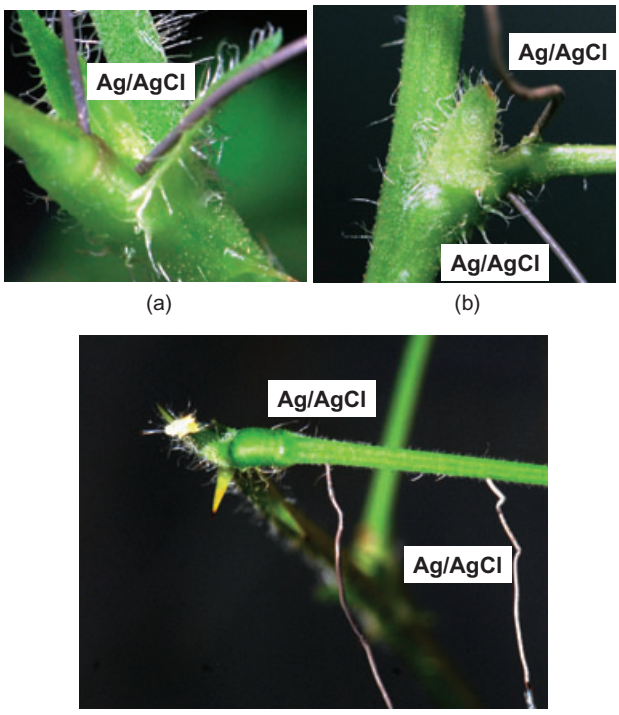

Figure 3. Location of electrodes in *Mimosa pudica*: (a) along a pulvinus, (b) across a pulvinus and (c) along a petiole.

The time dependencies of the charged capacitors discharging into the *M. pudica* through the electrodes that were at different positions in the pulvinus and the petiole are shown in Figs 4a–9a. Figures 4b–9b show the same dependencies in logarithmic coordinates.

Discharge of a 100 μF capacitor in the pulvinus caused the petiole to fall a few seconds after the start of discharge (Fig. 10) if the capacitor was charged from a 1.5 V battery. After the capacitor was disconnected from the Ag/AgCl electrodes, the petiole slowly relaxed back to the initial position as shown in Fig. 10a. If the electrodes are placed in the petiole, a higher voltage is required for the petiole to fall down. Yao *et al.* (2008) found that application of 9 V to the petiole caused the petiole to fall down.

Mathematical treatment of capacitor discharge

If a capacitor of capacitance C is discharged during time t through a resistor R (Fig. 11a), the logarithm of capacitor voltage U is

$$\log_{10} U(t) = \log_{10} U_0 - t/2.3\tau, \quad (1)$$

where U_0 is the initial voltage of a capacitor, and τ is the time constant. The circuit time constant RC governs the discharging process. At $\tau = RC$, the capacitor charge is

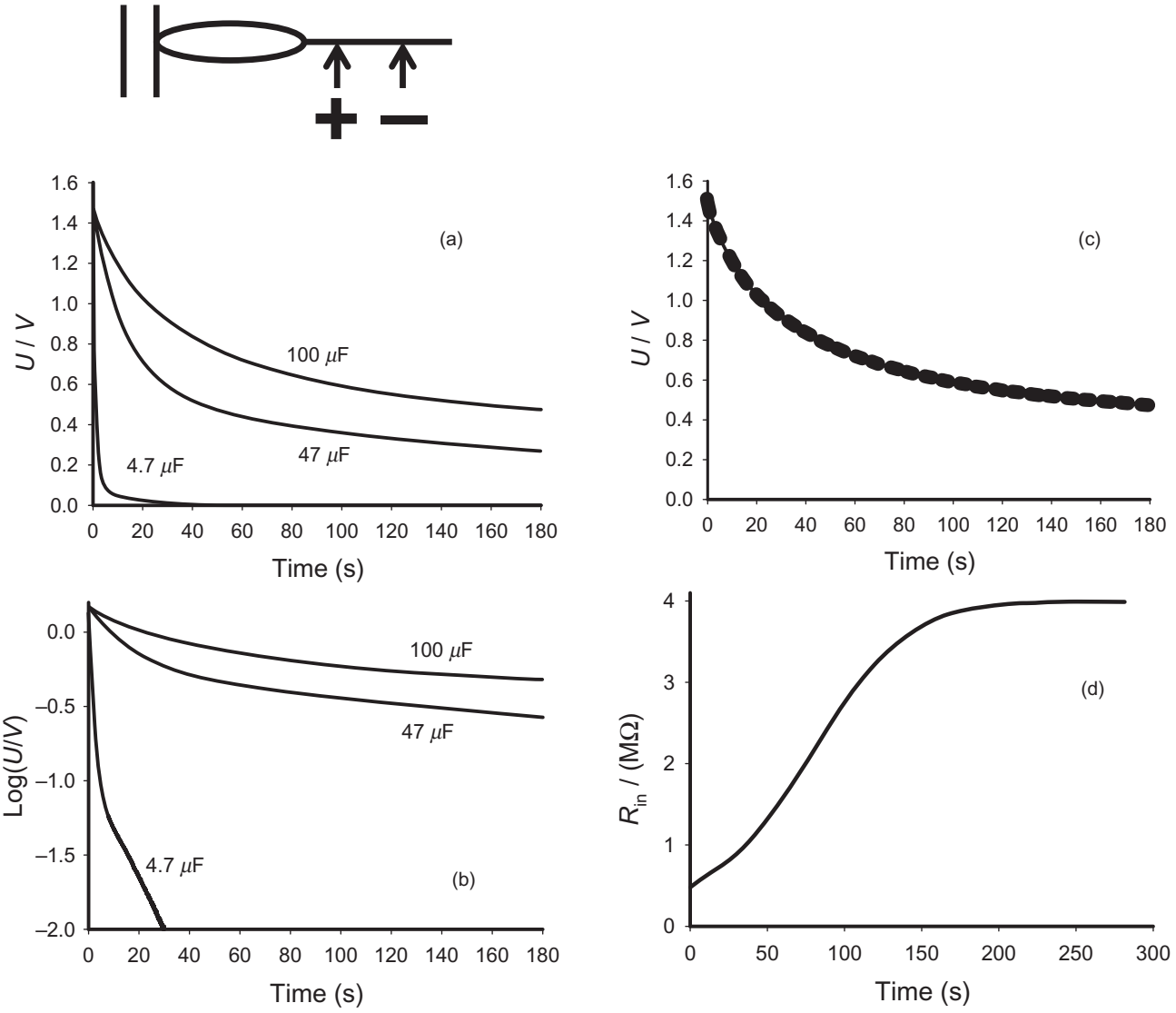

Figure 4. (a) Time dependence of electrical discharge in *Mimosa pudica* petiole between electrodes connected to charged capacitors and the PXI-4071 digital voltmeter. Location of Ag/AgCl electrodes is shown in Fig. 3c. (b) Time dependence of electrical discharge in the *M. pudica* petiole between electrodes connected to charged capacitors and the PXI-4071 digital voltmeter in logarithmic coordinates. (c) Time dependence of electrical discharge in *M. pudica* petiole between electrodes connected to 100 μF charged capacitor; dashed line – experiment, solid line is theoretical estimation from Eqns 4 and 5. (d) Time dependence of input resistance during discharge of charged capacitor in a petiole. *U* is the capacitor voltage in volts.

reduced to CU_0e^{-1}, which is about 37% of its initial charge. The voltage across the capacitor decreases exponentially from the initial value U_0 to zero. As the capacitance or resistance increases, the time of the capacitor discharge increases according to Eqn 1.

It was observed that capacitor discharge through the *M. pudica* petiole has a two-exponential character (Figs 4a & 5a). Therefore, the electrical circuit can be modelled as it is shown in Fig. 11b. In our experiment, the capacitor C_1 was charged to voltage U_0, and the circuit was closed.

After closing the circuit, the electrical potentials U_1 and U_2 at capacitors C_1 and C_2 depend on time according to the equations:

$$\begin{cases} C_1\dfrac{dU_1}{dt} = -\dfrac{1}{R_1}(U_1 - U_2) \\ C_2\dfrac{dU_2}{dt} = -\dfrac{1}{R_1}U_1 - \left(\dfrac{1}{R_1} + \dfrac{1}{R_2}\right)U_2, \end{cases} \quad (2)$$

with initial conditions

$$U_1[0] = U_0, \quad U_2[0] = 0, \quad (3)$$

It is convenient to introduce parameters of time:

$$\theta_1 = R_1C_1, \quad \theta_2 = R_2C_2, \quad \theta_3 = R_2C_1, \quad (4)$$

Voltage U_2 can be excluded from the system of Eqn 2, giving the single equation for U_1:

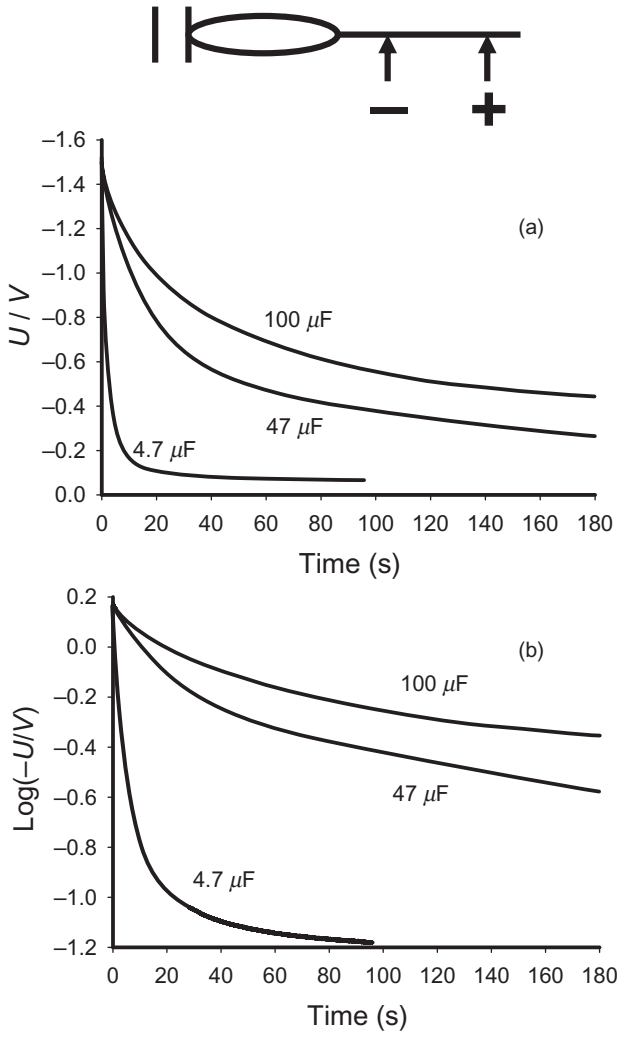

Figure 5. (a) Time dependence of electrical discharge in *Mimosa pudica* petiole between electrodes connected to a charged capacitor and the PXI-4071 digital voltmeter. (b) Time dependence of electrical discharge in the *M. pudica* petiole between electrodes connected to a charged capacitor and the PXI-4071 digital voltmeter in logarithmic coordinates. *U* is the capacitor voltage in volts.

$$\theta_1\theta_2\frac{\mathrm{d}^2U_1}{\mathrm{d}t^2}+(\theta_1+\theta_2+\theta_3)\frac{\mathrm{d}U_1}{\mathrm{d}t}+U_1=0, \tag{5}$$

Solving this equation, one can find the time course of U_1:

$$U_1(t)=U_0\left\{\left[\frac{-\theta_1+\theta_2-\theta_3}{\sqrt{-4\theta_1\theta_2+(\theta_1+\theta_2+\theta_3)^2}}+1\right]\right. \tag{6}$$
$$\mathrm{Exp}\left[-\frac{t\left(\theta_1+\theta_2+\theta_3+\sqrt{-4\theta_1\theta_2+(\theta_1+\theta_2+\theta_3)^2}\right)}{2\theta_1\theta_2}\right]+$$
$$\left[\frac{\theta_1-\theta_2+\theta_3}{\sqrt{-4\theta_1\theta_2+(\theta_1+\theta_2+\theta_3)^2}}+1\right]$$
$$\left.\mathrm{Exp}\left[-\frac{t\left(\theta_1+\theta_2+\theta_3-\sqrt{-4\theta_1\theta_2+(\theta_1+\theta_2+\theta_3)^2}\right)}{2\theta_1\theta_2}\right]\right\},$$

If the experimental dependence can be approximated with function

$$U(t)=A_1\mathrm{Exp}\left[-\frac{t}{\tau_1}\right]+A_2\mathrm{Exp}\left[-\frac{t}{\tau_2}\right], \tag{7}$$

and parameters A_1, A_2, τ_1 and τ_2 can be determined from the experiment (Fig. 4a), then one can evaluate the elements of the equivalent circuit in Fig. 11b.

To find parameters θ_1, θ_2, θ_3 simultaneously, we need to solve the set of non-linear equations derived from comparison of Eqns 6 and 7:

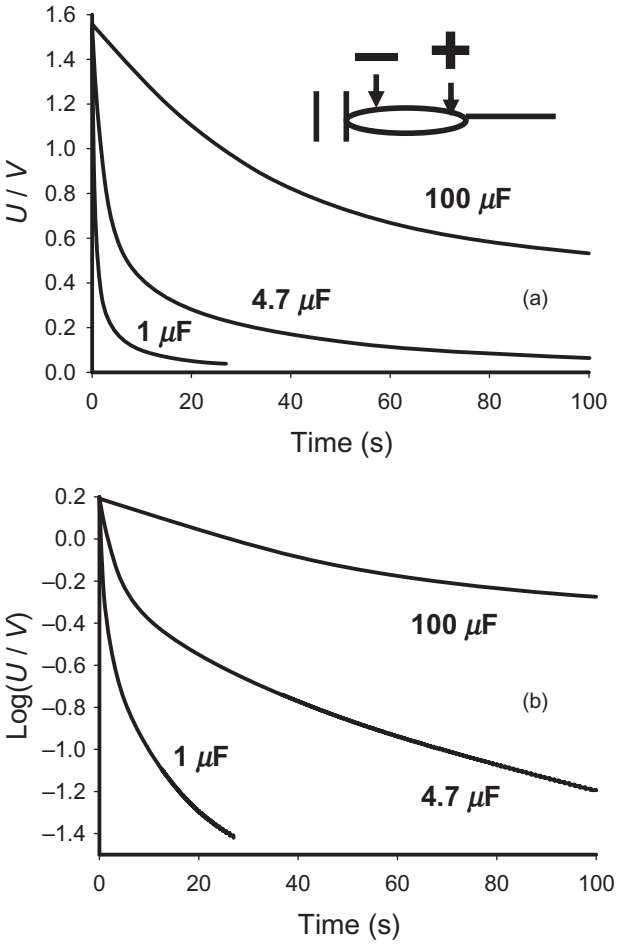

Figure 6. (a) Time dependence of electrical discharge in *Mimosa pudica* pulvinus between electrodes connected to charged capacitors and the PXI-4071 digital voltmeter. (b) Time dependence of electrical discharge in the *M. pudica* petiole between electrodes connected to charged capacitors and the PXI-4071 digital voltmeter in logarithmic coordinates. *U* is the capacitor voltage in volts.

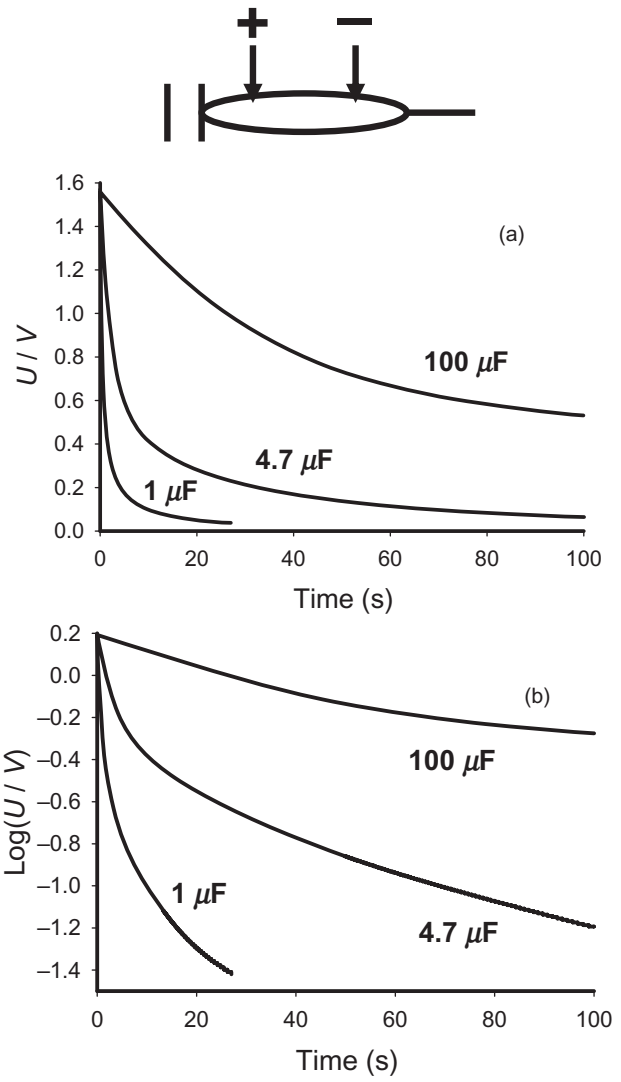

Figure 7. (a) Time dependence of electrical discharge in the *Mimosa pudica* pulvinus between electrodes connected to a charged capacitor and the PXI-4071 digital voltmeter. (b) Time dependence of electrical discharge in *M. pudica* pulvinus between electrodes connected to a charged capacitor and the NI-PXI-4071 digital voltmeter in logarithmic coordinates.

$$A_1 = U_0\left[\frac{-\theta_1+\theta_2-\theta_3}{\sqrt{-4\theta_1\theta_2+(\theta_1+\theta_2+\theta_3)^2}}+1\right] \quad (8)$$

$$\frac{1}{\tau_1} = \frac{\theta_1+\theta_2+\theta_3+\sqrt{-4\theta_1\theta_2+(\theta_1+\theta_2+\theta_3)^2}}{2\theta_1\theta_2}$$

$$\frac{1}{\tau_2} = \frac{\theta_1+\theta_2+\theta_3-\sqrt{-4\theta_1\theta_2+(\theta_1+\theta_2+\theta_3)^2}}{2\theta_1\theta_2},$$

Finding from here θ_1, θ_2 and θ_3, and using the set of Eqn 4, one can determine the value of elements C_2, R_1, R_2 in the equivalent circuit (Fig. 11b).

Another interesting parameter is input resistance that can be defined as

$$R_{\text{input}} = -U_1 \Big/ C_1\frac{dU_1}{dt}, \quad (9)$$

This parameter is often analysed in electrical impedance spectroscopy studies of biological tissues (Zhang & Willison 1991; Wang, Zimmermann & Benz 1994; Laarabi *et al.* 2005). However, there is a problem with interpretation of electrical impedance analysis, because a few different equivalent circuit models can have identical impedances.

Calculating circuit parameters

In Fig. 4, we used capacitance $C_1 = 100\ \mu$F and $U_0 = 1.5$ V. Experimental measurements provided the discharge curve given in Fig. 4c by the dashed line. Solving Eqn 5, we found characteristic times

$\theta_1 = 52.42$ s, $\theta_2 = 207.90$ s, $\theta_3 = 166.92$ s

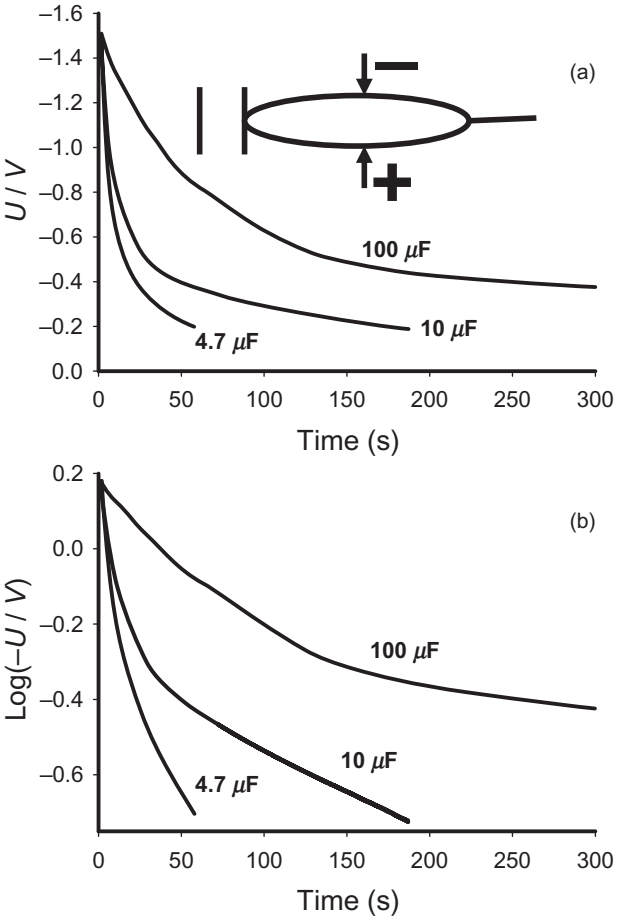

Figure 8. (a) Time dependence of electrical discharge in the *Mimosa pudica* pulvinus between electrodes connected to charged capacitors and the NI-PXI-4071 digital voltmeter. (b) Time dependence of electrical discharge in the *M. pudica* pulvinus between electrodes connected to charged capacitors and the PXI-4071 digital voltmeter in logarithmic coordinates.

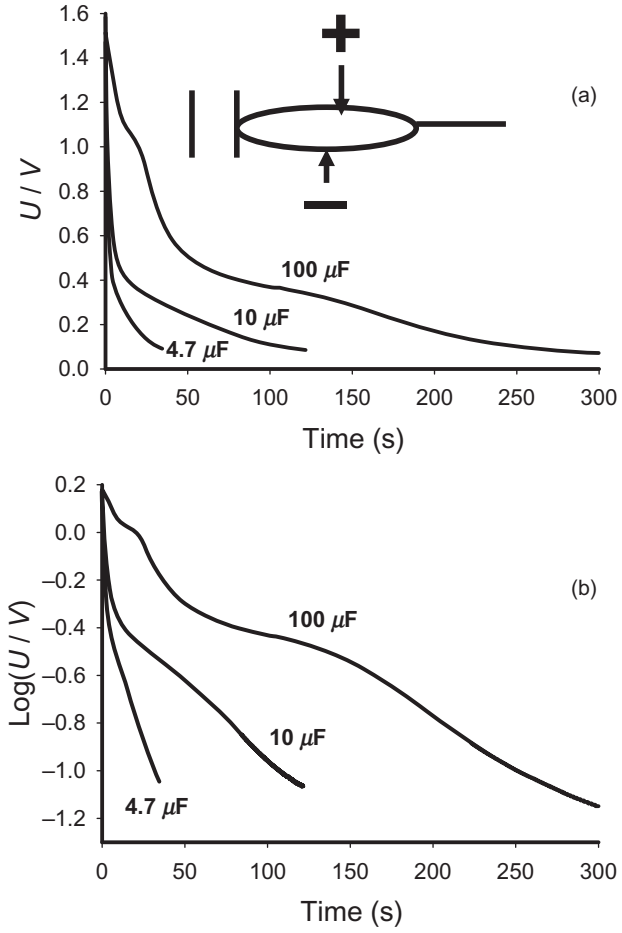

Figure 9. (a) Time dependence of electrical discharge in *Mimosa pudica* pulvinus between electrodes connected to a charged capacitor and the PXI-4071 digital voltmeter. (b) Time dependence of electrical discharge in the *M. pudica* pulvinus between electrodes connected to a charged capacitor and the NI-PXI-4071 digital voltmeter in logarithmic coordinates.

and from Eqn 4, we found the capacitance and the resistances in the equivalent circuit:

$$R_1 = 0.542\ \mathrm{M}\Omega, C_2 = 124.552\ \mu\mathrm{F}, R_2 = 1.6692\ \mathrm{M}\Omega$$

Using these parameters, we calculated the theoretical curve (solid line), and superimposed it on the experimental curve in Fig. 4c. The two curves merged completely. We calculated the input resistance presented in Fig. 4d. As one can see, input resistance increases from 0.52 to 4.0 MΩ. We also studied a few different capacitors discharging through the same plant tissues. The results for $C_1 = 100$, 47 and 4.7 μF are presented in Fig. 12 by solid lines. The calculated time-course of voltage at these capacitors based on the electrical circuit shown in Fig. 11b was represented here by dashed lines. One can see rather close agreement between the predicted and observed values.

DISCUSSION

Electrical circuits in a petiole

We have analysed the discharge of the capacitor through the petiole of *M. pudica*. The goal was to elucidate the structure of the biologically closed electrical circuits in *M. pudica*. We started with a capacitor of 100 μF, and found that its discharge of 1.5 V could be ideally modelled by a simple electrical circuit shown in Fig. 11b.

The initial voltages applied from the charged 4.7 μF capacitor were $\pm$1.5, $\pm$1.0 and $\pm$0.5 V, and we found that these curves ideally scale to the initial one (Fig. 13). That proves that the electrical circuit in petiole between electrodes is the passive one and does not depend on voltage.

We also studied capacitors of different values, and calculated expected discharge curves presented in Fig. 12. We presumed that the electrical circuit should remain the same. Although the predicted and observed curves are rather close to each other, there is a certain discrepancy. The reason could be that the equivalent electrical circuit shown in Fig. 11b is too simplified, and the actual circuit has a different and rather distributed character.

We measured the input resistance, and found that it changes with time and voltage on the discharging capacitor. This is a common feature in biological structures and usually is explained by the opening of ion channels in cellular membranes when input resistance decreases. In our

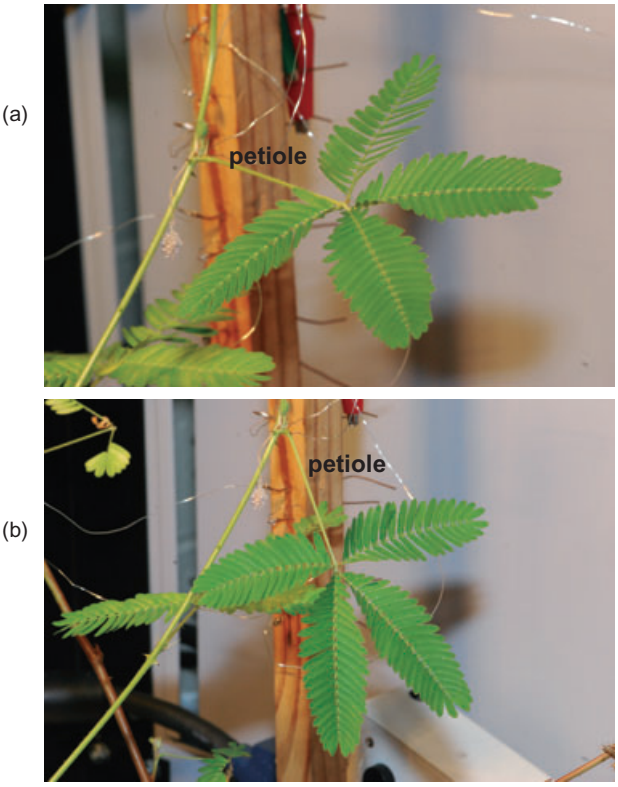

Figure 10. The petiole (a) falls down (b) in response to an electrical discharge of a 100 μF capacitor in a pulvinus in a few seconds.

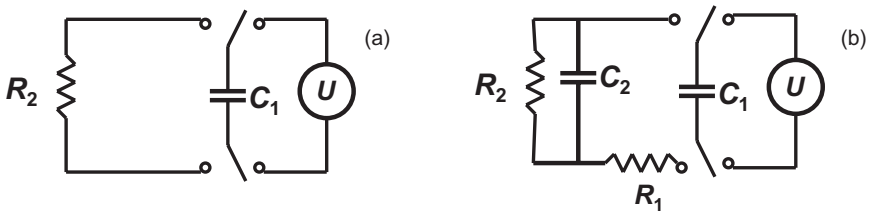

Figure 11. Electrical equivalent schemes of a capacitor discharge in a plant tissue. Abbreviations: C_1, charged capacitor from voltage source U; C_2, capacitance of plant tissue; R, resistance in the *Mimosa pudica* tissue.

case, it was increasing because of charging of the effective capacitor C_2 inside the tissue. We found the value of this capacitor to be 124 μF. It is close to the testing capacitor $C_1 = 100$ μF.

Biologically closed electrical circuits operate over large distances in biological tissues (Nordestrom 1983; Volkov *et al.* 2009a,b). Figures 4–9 show experimental dependencies of voltage of various charged capacitors on time. Logarithmic dependencies in Figs 4b–9b show significant deviations from the linear prediction of Eqn 1. Such deviations cannot be described by the equivalent scheme shown in Fig. 11a.

Electrical circuits in a pulvinus

The equivalent electrical circuits shown in Fig. 11a,b predict the independence of the results on the polarity of the electrodes during a capacitor discharge in the pulvinus of *M. pudica*. Changing the polarity of the electrodes leads to different results in the kinetics of the capacitor discharge (Figs 6–9). This effect is similar to the electrical discharge in the Venus flytrap, and is caused by the opening of voltage-gated ion channels (Volkov *et al.* 2009a,b,c). Figure 14 shows time dependencies of a 100 μF discharge in a pulvinus when the polarity of the electrodes is reversed. There is a strong rectification effect in the kinetics of the discharge of the capacitor. The same results were received in control experiments using Pt electrodes instead of Ag/AgCl electrodes.

It is convenient to represent electrochemical properties of biologically closed electrical circuits with idealized equivalent electrical circuit models consisting of discrete electrical components. We can simulate the voltage-gated K^+- and Ca^{2+}-permeable Cl^- ion channels by diodes. Figures 8, 9 and 14 show a very large deviation from Eqn 1, as well as unusual slopes and changing curvatures in the time dependencies of the capacitor's discharge. Figures 8a and 9a show different kinetics of capacitors discharging between the same electrodes in the pulvinus after the polarity on the capacitors was changed. There is a strong rectification effect inside a pulvinus sensitive to the polarity of the capacitors (Figs 8a, 9a & 14). This can be caused by a redistribution of K^+, Cl^- and Ca^{2+} ions through ion channels in the pulvinus.

The activation of biologically closed electrical circuits in *M. pudica* can lead to different responses in plant tissue. A mechanical or electrical stimulus can induce electrical signals or action potentials, which propagate along the plasma membrane in a phloem. Nerve cells in animals and phloem cells in plants share one fundamental property: they possess excitable membranes through which electrical excitations in the form of action potentials can propagate.

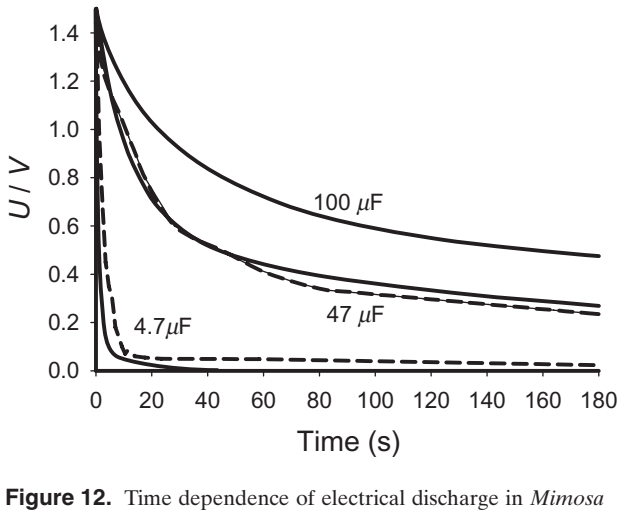

Figure 12. Time dependence of electrical discharge in *Mimosa pudica* petiole between electrodes connected to charged capacitors and the PXI-4071 digital voltmeter. Location of Ag/AgCl electrodes is shown in Fig. 3c. Solid lines are experimental, and dashed lines are theoretical dependencies.

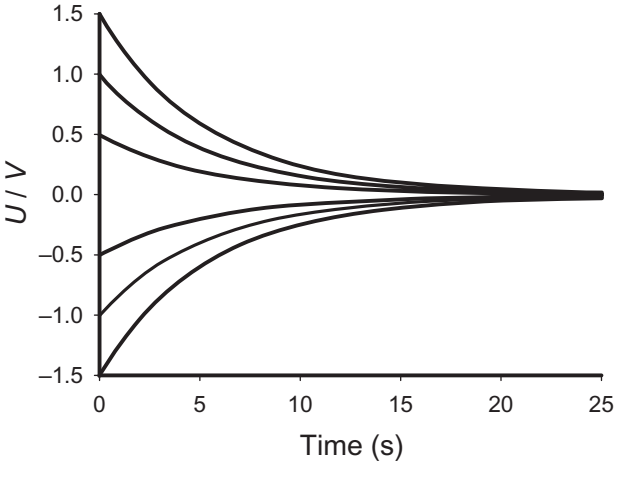

Figure 13. Time dependence of electrical discharge in *Mimosa pudica* petiole between electrodes connected to 4.7 μF charged capacitor and the PXI-4071 digital voltmeter. The initial voltages applied from the charged capacitor were ± 1.5, ± 1.0 and ± 0.5 V. Location of Ag/AgCl electrodes is shown in Fig. 3c. U is the capacitor voltage in volts.

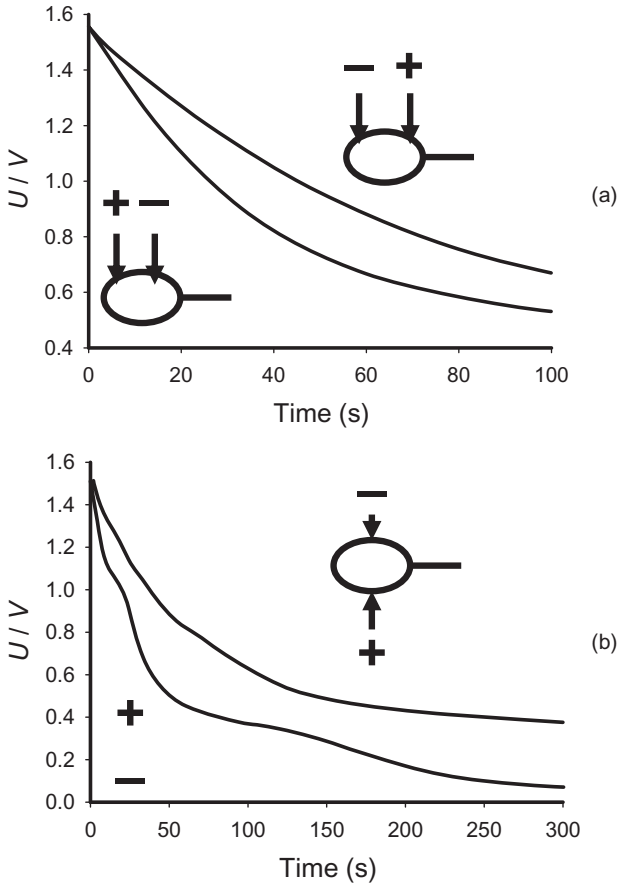

Figure 14. Time dependence of electrical discharge in the *Mimosa pudica* pulvinus between electrodes connected to 100 μF charged capacitor and the PXI-4071 digital voltmeter.

These propagating excitations are modelled theoretically as travelling wave solutions of certain parameter-dependant non-linear reaction–diffusion equations coupled with some non-linear ordinary differential equations. The plasma membranes in phloem cells facilitate the passage of electrical excitations in the form of action potentials. The internal functioning of a plant can be maintained and developed in a continuously varying environment only if all cells, tissues and organs function in concordance (Trewavas 2003, 2005). Voltage-gated ionic channels control the plasma membrane potential and the movement of ions across membranes, thereby regulating various biological functions. These biological nanodevices play vital roles in signal transduction in higher plants. Propagation of action potentials in *M. pudica* along the petioles and pulvini, and in the stem is documented in literature (Houwink 1935; Umrath 1937; Sibaoka 1962).

Propagation of an action potential can induce a mechanical response by activating the H^+-ATPase (Liubimova-Engel'gardt *et al.* 1978), calcium-permeable Cl^- channel (Abe 1981) and/or the voltage-gated K^+ ion channel in a pulvinus (Samejima & Sibaoka 1982). Redistribution of ions between the upper and lower parts of a pulvinus induces fast transport of water through aquaporins, and causes a fast change in the volume of the motor cells. Voltage-gated K^+ and Cl^- ion channels can operate as an electrical starter of the osmotic motor in a pulvinus. Ion fluxes activate fast water transport through aquaporins between the lower half of the pulvinus and the upper half of the pulvinus following an electrical stimulus.

ACKNOWLEDGMENT

This work was supported by the National Science Foundation (grant no. HRD0811507).

REFERENCES

Abe T. (1980) The shortening and action potential of the cortex in the main pulvinus of *Mimosa pudica*. *Botanical Magazine Tokyo* **93,** 247–251.

Abe T. (1981) Chloride ion efflux during an action potential in the main pulvinus of *Mimosa pudica*. *Botanical Magazine Tokyo* **94,** 379–383.

Abe T. & Oda K. (1976) Resting and action potentials of excitable cells in the main pulvinus of *Mimosa pudica*. *Plant & Cell Physiology* **17,** 1343–1346.

Balmer R.T. & Franks J.G. (1975) Contractile characteristics of *Mimosa pudica* L. *Plant Physiology* **56,** 464–467.

Barlow P.W. (2008) Reflections on 'plant neurobiology'. *Biosystems* **92,** 132–147.

Bertholon M. (1783) *De L'electricite Des Vegetaux: Ouvrage Dans Lequel on Traite De L'electricite De L'atmosphere Sur Les Plantes, De Ses Effets Sur Leconomie Des Vegetaux, De Leurs Vertus Medico*. P.F. Didot Jeune, Paris, France.

Bose J.C. (1902) *Response in Living and Non-Living*. Longmans Green, London, UK.

Bose J.C. (1907) *Comparative Electrophysiology*. Longmans Green, London, UK.

Bose J.C. (1913) *Researches on Irritability of Plants*. Longmans Green, London, UK.

Bose J.C. (1918) *Movements in Plants*. B.R. Publishing Corp., Delhi, India.

Bose J.C. (1926) *The Nervous Mechanism of Plants*. Longmans-,Green & Co., London, UK.

Bose J.C. (1928) *The Motor Mechanism of Plants*. Longmans Green, London, UK.

Bulychev A.A., Niyazova M.M. & Turovetsky V. (1986) Electroinduced changes of chlorophyll fluorescence in individual intact chloroplasts. *Biochimica et Biophysica Acta* **850,** 218–225.

Darwin C. (1875) *Insectivorous Plants*. Murray, London, UK.

Eschrich W. (1989) *Stofftransport in Bäumen*. Sauerländer, Frankfurt, Germany.

Fleurat-Lessard P., Bouche-Pillion S., Leloup C. & Bonnemain J. (1997) Distribution and activity of the plasma membrane H^+-ATPase related to motor cell function in *Mimosa pudica* L. *Plant Physiology* **114,** 827–834.

Fromm J. (1991) Control of phloem unloading by action potentials in *Mimosa*. *Physiologia Plantarum* **83,** 529–533.

Fromm J. & Eschrich W. (1988) Transport processes in stimulated and non-stimulated leaves of *Mimosa pudica*. *Trees* **2,** 18–24.

Fromm J. & Lautner S. (2007) Electrical signals and their physiological significance in plants. *Plant, Cell & Environment* **30,** 249–257.

Houwink A.L. (1935) The conduction of excitation in *Mimosa pudica*. *Recuril des Travaux Botaniques Neerlandais* **32,** 51–91.

Houwink A.L. (1938) The conduction of excitation in *Clematis zeylanica* and in *Mimosa pudica*. *Annales du Jardin Botanique de Buitenzorg* **48,** 10–16.

Kagawa H. & Saito E. (2000) A model of main pulvinus movement of *Mimosa pudica*. *JSME International Journal* **43,** 923–928.

Kaiser H. & Grams T. (2006) Rapid hydropassive opening and subsequent active stomatal closure follow heat-induced electrical signals in *Mimosa pudica*. *Journal of Experimental Botany* **57,** 2087–2092.

Kameyama K., Kishi Y., Yoshomura M., Kanzawa N. & Tsuchia T. (2000) Thyrosine phosphorylation in plant bending. *Nature* **407,** 37.

Koziolek C., Grams T.E.E., Schreiber U., Matyssek R. & Fromm J. (2003) Transient knockout of photosynthesis mediated by electrical signals. *New Phytologist* **161,** 715–722.

Ksenzhek O.S. & Volkov A.G. (1998) *Plant Energetics*. Academic Press, San Diego, CA, USA.

Laarabi S., Kinani K.E., Ettouhami A. & Limouri M. (2005) *In vivo* impedance of the aerial organs of some mono- and dicotyledonous plants. *Comptes Rendus Biologies* **328,** 253–262.

Lang R.D. & Volkov A.G. (2008) Solitary waves in soybean induced by localized thermal stress. *Plant Signaling & Behavior* **3,** 224–228.

Liubimova M.N., Deminovskaya N.S. & Fedorovich I.B. (1964) The part played by ATP in the motor function of *Mimosa pudica* leaf. *Biokhimia (Moscow)* **29,** 774–779.

Liubimova-Engel'gardt M.N., Burnasheva S.A., Fain F.S., Mitina N.A. & Poprykina I.M. (1978) *Mimosa pudica* adenosine triphosphatase. *Biokhimia (Moscow)* **439,** 748–760.

Malone M. (1994) Wound-induced hydraulic signals and stimulus transmission in *Mimosa pudica* L. *New Phytologist* **128,** 49–56.

Malone M. (1996) Rapid long-distance signal transmission in higher plants. *Advances in Botanical Research* **22,** 163–228.

Markin V.S. & Sachs F. (2004) Thermodynamics of mechanosensitivity. *Physical Biology* **1,** 110–124.

Markin V.S., Volkov A.G. & Jovanov E. (2008) Active movements in plants: mechanism of trap closure by *Dionaea muscipula* Ellis. *Plant Signaling & Behavior* **3,** 778–783.

Nordestrom B.E.W. (1983) *Biologically Closed Electrical Circuits. Clinical, Experimental and Theoretical Evidence for an Additional Circulatory System*. Nordic Medical Publications, Uppsala, Sweden.

Oda K. & Abe T. (1972) Action potential and rapid movement in the main pulvinus of *Mimosa pudica*. *Botanical Magazine Tokyo* **85,** 135–145.

Pikulenko M.M. & Bulychev A.A. (2005) Light-triggered action potentials and changes in quantum efficiency of photosystem II in *Anthoceros* cells. *Russian Journal of Plant Physiology* **52,** 660–666.

Ricca U. (1916) Soluzione d'un problema di fisiologia. La propagazione di stimulo nella '*Mimosa*'. *Nuovo Giornale Botanico Italiano Nuovo Serie* **23,** 51–170.

Roblin G. (1979) *Mimosa pudica*: a model for the study of the excitability in plants. *Biology Reviews* **54,** 135–153.

Roblin G. (1982) Movements, bioelectrical events and proton excretion induced in the pulvini of *Mimosa pudica* L. by a period of darkness. *Zeitschrift fur Pflanzenphysiologie* **108,** 295–304.

Roblin G. & Fleurate-Lessard P. (1987) Redistribution of potassium, chloride and calcium during the gravitropically induced movement of *Mimosa pudica* pulvinus. *Planta* **170,** 242–248.

Samejima M. & Sibaoka T. (1982) Membrane potentials and resistance of excitable cells in the petiole and main pulvinus of *Mimosa pudica*. *Plant & Cell Physiology* **23,** 459–465.

Shimmen T. (2006) Electrophysiology in mechanosensing and wounding response. In *Plant Electrophysiology – Theory & Methods* (ed. A.G. Volkov), pp. 319–339. Springer-Verlag, Berlin and Heidelberg, Germany.

Sibaoka T. (1962) Excitable cells in *Mimosa*. *Science* **137,** 226.

Sibaoka T. (1966) Action potentials in plant organs. *Symposia of the Society for Experimental Biology* **20,** 49–74.

Sibaoka T. (1969) Physiology of rapid movements in higher plants. *Annual Reviews of Plant Physiology* **20,** 165–184.

Sibaoka T. (1991) Rapid plant movements triggered by action potentials. *Botanical Magazine Tokyo* **104,** 73–95.

Stoeckel H. & Takeda K. (1993) Plasmalemmal, voltage-dependent ionic currents from excitable pulvinar motor cells of *Mimosa pudica*. *Journal of Membrane Biology* **131,** 179–192.

Tamiya T., Miyasaki T., Ishikawa H., Iruguchi N., Maki T., Matsumoto J.J. & Tsuchiya T. (1988) Movement of water in conjunction with plant movement visualized by NMR imaging. *Journal of Biochemistry* **104,** 5–8.

Temmei Y., Uchida S., Hoshino D., Kanzawa N., Kuwahara M., Sasaki S. & Tsuchia T. (2005) Water channel activities of *Mimosa pudica* plasma membrane intrinsic proteins are regulated by direct interaction and phosphorylation. *FEBS Letters* **579,** 4417–4422.

Tinz-Füchtmeier A. & Gradmann D. (1990) Laser-interferometric re-examination of rapid conductance of excitation in *Mimosa pudica*. *Journal of Experimental Botany* **41,** 15–19.

Trewavas A. (2003) Aspects of plant intelligence. *Annals of Botany* **92,** 1–20.

Trewavas A. (2005) Green plants as intelligent organisms. *Trends in Plant Science* **10,** 413–419.

Umrath K. (1937) Der Erregungsvorgang bei höheren Pflanzen. *Ergebnisse der Biologie* **14,** 1–142.

Volkov A.G. (2000) Green plants: electrochemical interfaces. *Journal of Electroanalytical Chemistry* **483,** 150–156.

Volkov A.G. (2006a) Electrophysiology and phototropism. In *Communication in Plants. Neuronal Aspects of Plant Life* (eds F. Balushka, S. Manusco & D. Volkman), pp. 351–367. Springer-Verlag, Berlin, Germany/New York, NY, USA.

Volkov A.G. (ed.) (2006b) *Plant Electrophysiology*. Springer-Verlag, Berlin, Germany.

Volkov A.G. & Brown C.L. (2006a) Electrochemistry of plant life. In *Plant Electrophysiology – Theory & Methods* (ed. A.G. Volkov), pp. 437–459. Springer-Verlag, Berlin, Germany.

Volkov A.G. & Brown C.L. (2006b) Nanodevices in nature. In *Nanodevices for Life Sciences* (ed. C.S.S.R. Kumar), pp. 440–463. Wiley-VCH, Weinheim, Germany.

Volkov A.G. & Haack R.A. (1995) Insect induces bioelectrochemical signals in potato plants. *Bioelectrochemistry and Bioenergetics* **35,** 55–60.

Volkov A.G., Adesina T., Markin V.S. & Jovanov E. (2007) Closing of Venus flytrap by electrical stimulation of motor cells. *Plant Signaling & Behavior* **2,** 139–144.

Volkov A.G., Adesina T., Markin V.S. & Jovanov E. (2008a) Kinetics and mechanism of *Dionaea muscipula* trap closing. *Plant Physiology* **146,** 694–702.

Volkov A.G., Coopwood K.J. & Markin V.S. (2008b) Inhibition of the *Dionaea muscipula* Ellis trap closure by ion and water channels blockers and uncouplers. *Plant Science* **175,** 642–649.

Volkov A.G., Carrell H., Adesina T., Markin V.S. & Jovanov E. (2008c) Plant electrical memory. *Plant Signaling & Behavior* **3,** 490–492.

Volkov A.G., Carrell H., Baldwin A. & Markin V.S. (2009a) Electrical memory in Venus flytrap. *Bioelectrochemistry* **75,** 142–147.

Volkov A.G., Carrell H. & Markin V.S. (2009b) Biologically closed electrical circuits in Venus flytrap. *Plant Physiology* **149,** 1661–1667.

Volkov A.G., Carrell H. & Markin V.S. (2009c) Molecular electronics of the *Dionaea muscipula* trap. *Plant Signaling & Behavior* **4,** 353–354.

Wang J., Zimmermann U. & Benz R. (1994) Contribution of electrogenic ion transport to impedance of the algae *Valonia utricularis* and artificial membranes. *Biophysical Journal* **67,** 1582–1593.

Yao H., Xu Q. & Yuan M. (2008) Actin dynamics mediates the changes of calcium level during the pulvinus movement of *Mimosa pudica*. *Plant Signaling & Behavior* **3,** 954–960.

Zhang M.I.N. & Willison J.H.M. (1991) Electrical impedance analysis in plant tissues: a double shell model. *Journal of Experimental Botany* **42,** 1465–1475.

Received 1 November 2009; accepted for publication 5 December 2009